Optimized scattering compensation for time-of-flight camera

James Mure-Dubois and Heinz Hügli

University of Neuchâtel - Institute of Microtechnology, 2000 Neuchâtel, Switzerland

ABSTRACT

Recent time-of-flight (TOF) cameras allow for real-time acquisition of range maps with good performance. However, the accuracy of the measured range map may be limited by secondary light reflections. Specifically, the range measurement is affected by scattering, which consists in parasitic signals caused by multiple reflections inside the camera device. Scattering, which is particularly strong in scenes with large aspect ratios, must be detected and the errors compensated. This paper considers reducing scattering errors by means of image processing methods applied to the output image from the time-of-flight camera. It shows that scattering reduction can be expressed as a deconvolution problem on a complex, two-dimensional signal. The paper investigated several solutions. First, a comparison of image domain and Fourier domain processing for scattering compensation is provided. One key element in the comparison is the computation load and the requirement to perform scattering compensation in real-time. Then, the paper discusses strategies for improved scattering reduction. More specifically, it treats the problem of optimizing the description of the inverse filter for best scattering compensation results. Finally, the validity of the proposed scattering reduction method is verified on various examples of indoor scenes.

Keywords: 3D vision, time-of-flight, range imaging, scattering, deconvolution, range camera

1. INTRODUCTION

Recent time-of-flight (TOF) cameras allow for real-time acquisition of range maps with good performance. For instance, the Swissranger SR-3000 camera has a 176×144 pixels sensor, and supports continuous operation at 20 Hz.[1] The depth resolution can be better than 1 cm in favourable conditions, i.e. with no bright light sources in the field of view.[2] However, depth measurement is degraded by scattering, which consists in secondary reflections occurring between the lens and the imager[3,4,.5]The degradation is particularly strong when the weak signal from far objects (background) is affected by the strong scattering signal from foreground objects. This degradation of the depth image is a significant penalty in many applications, especially when background subtraction methods are employed.[3] For this reason, scattering must be suppressed, or at least reduced.

In [5], scattering reduction was expressed as a deconvolution problem on a complex, two-dimensional signal. The proposed algorithm for scattering reduction uses inverse filters implemented by a sum of separable gaussians. In this paper, we will discuss two improvements to this approach. The first improvement is the usage of Fourier domain processing for convolution operations. Processing in Fourier domain brings the advantage that the computation time per frame is significantly shorter than for spatial filtering. The second contribution concerns the degradation modeling. Given that an accurate measurement of the PSF is not possible, the paper considers various possible descriptions for the scattering. Finally, parametric models where the scattering degradation is expressed as a sum of gaussian filters are used. A method for parameter estimation is described that opens to the automatic determination of a camera specific scattering compensation model.

The remainder of this paper is organized as follows. A brief reminder of time-of-flight imaging principles is presented in section 2. Section 3 discusses image domain versus Fourier domain processing. The different descriptions for usable scattering models are discussed in section 4. Finally, section 5 presents real-world results illustrating the performance of scattering compensation.

2. TIME-OF-FLIGHT IMAGING AND SCATTERING

State-of-the-art TOF cameras[6,7,8]are based on the continuous emission of a periodic signal. The frequency of modulation f of this signal is typically 20MHz. As the periodic signal received at each pixel (i,j) of the camera sensor is described by its amplitude $A(i,j)$ and its phase $\varphi(i,j)$, it can be expressed as a complex signal $S(i,j)$. The range r is directly proportional to the phase. With c as the speed of light, we have :

$$S(i,j) = A(i,j) \cdot e^{j\varphi(i,j)} \qquad r(i,j) = \frac{c}{4\pi f} \cdot \varphi(i,j) \tag{1}$$

Figure 1 shows an example of range image acquisition for a scene of an office room (1**(a)**). The TOF range data was acquired with a SR-3100 camera, and is represented in fig. 1**(b)** as a color coded image, between 0 and 7.5m

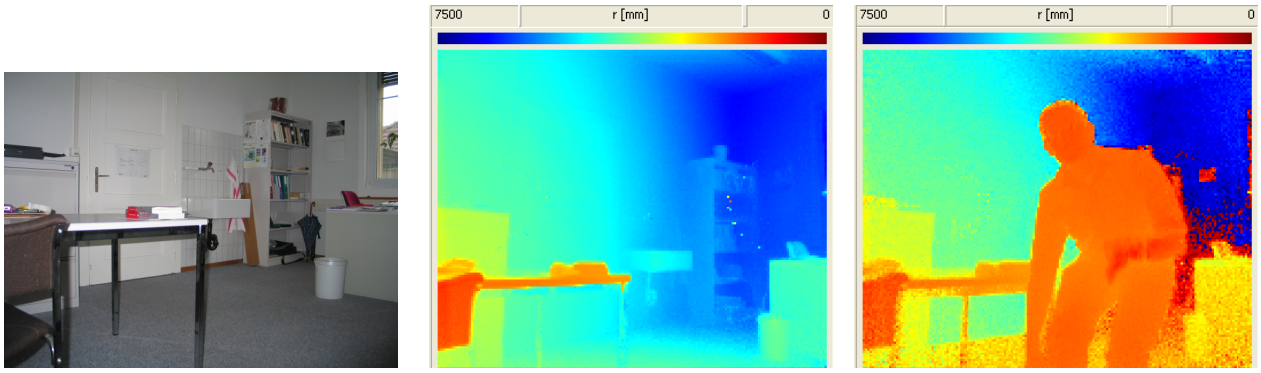

(a) Background : color image **(b)** Background : range image **(c)** Foreground : range image

Figure 1. TOF range images and scattering effects

To illustrate scattering, figure 1**(c)** shows the results of the depth measurement when a foreground object (in this case a person) is introduced in the field of view. Comparison of fig. 1**(b)** and 1**(c)** allows to identify changes in the background, which we will refer to as *scattering* artifacts.

The main mechanism behind scattering artifacts is a parasitic optical coupling between distinct pixels[1] . This coupling is caused by unwanted reflections on the camera sensor and optics, as illustrated schematically in fig.2. Based on this simple picture, a mathematical model for scattering was defined in [5]. This model is briefly summarized below. $S(i,j)$ is defined as the ideal signal entering the camera device and $S_{meas}(i,j)$ as the output signal delivered by the camera. The first assumption in the scattering model is that scattering can be described as an additive perturbation on the original signal, so that we have :

$$S_{meas}(i,j) = S(i,j) + S_{scat}(i,j) \tag{2}$$

where $S_{scat}(i,j)$ is the scattering signal due to parasitic reflections. The second assumption in the model is that scattering effects are linear, and similar for each position on the sensor, so that the scattering signal $S_{scat}(i,j)$ can be expressed as the result of the convolution of the ideal signal with a scattering PSF $\Delta h(i,j)$, i.e.

$$S_{scat}(i,j) = S(i,j) * *\Delta h(i,j) \tag{3}$$

If we define $\mathbf{h_0}$ as the neutral element with respect to convolution, we can express equation 2 with a convolution operation :

$$S_{meas}(i,j) = S(i,j) * *(h_0(i,j) + \Delta h(i,j)) = S(i,j) * *h(i,j) \tag{4}$$

where $\mathbf{h} = \mathbf{h_0} + \mathbf{\Delta h}$ is interpreted as a camera point spread function including scattering coupling.

In the following sections, we will see how this model for scattering can be used to implement scattering compensation, and how the knowledge of $\Delta h(i,j)$ is sufficient to implement a scattering compensation algorithm coherent with this model.

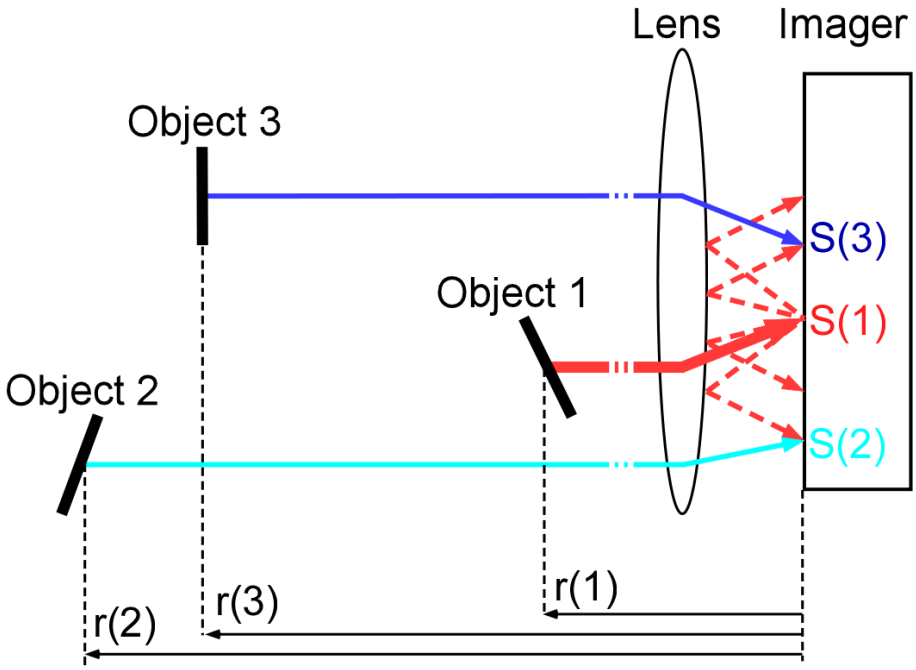

Figure 2. Light scattering in TOF camera .

3. SCATTERING COMPENSATION

The goal of scattering compensation is to remove artifacts caused by scattering in the depth images. Thus, scattering compensation can be interpreted as recovering the ideal signal $\mathbf{S}$ for each corresponding camera measurement $\mathbf{S_{meas}}$.

3.1. Deconvolution problem

Scattering compensation is indeed a deconvolution problem, since the signal $\mathbf{S}$ and $\mathbf{S_{meas}}$ are related by a convolution operation ($\mathbf{S_{meas}} = \mathbf{S} * *\mathbf{h}$), and that the final goal is to reconstruct $\mathbf{S}$ from the measurement $\mathbf{S_{meas}}$. In the following, we consider and compare two possible implementations of a deconvolution algorithm realized through standard image processing techniques. In the first implementation, the deconvolution is realized as a *spatial convolution* with an inverse filter $\mathbf{I}$, whereas in the second approach, the deconvolution is performed through a *division* in the *Fourier space*.

3.2. Image domain filtering

In the image domain filtering approach,[5] the data processing for scattering compensation is realized by applying an ad-hoc filter $\mathbf{I}$ on the measured image $\mathbf{S_{meas}}$. The result of the filtering operation is considered as the scattering free image data:

$$\mathbf{S} = \mathbf{S_{meas}} * *\mathbf{I} \tag{5}$$

Using again $\mathbf{h_0}$, the neutral element with respect to convolution, we can define the scattering correction response $\mathbf{\Delta I}$ so that $\mathbf{S_{scat}} = \mathbf{S} * *\mathbf{\Delta I}$. As stated in 5, the knowledge of $\mathbf{\Delta h}$ or $\mathbf{\Delta I}$ is equivalent, since those two filters are linked through the Fourier transform :

$$\mathbf{I} = \mathbf{h_0} - \mathbf{\Delta I} = \mathscr{F}^{-1}\left\{1/\mathscr{F}\left\{\mathbf{h_0} + \mathbf{\Delta h}\right\}\right\} \tag{6}$$

Image domain filtering is straightforward to implement, and can be advantageous when the filter employed is small (less than 10 pixels). However, the experience shows that, for scattering compensation, the filters used must be large (even larger that the image). The inverse filter method is then computation intensive. It should be used only in special cases of small filters , or when using separable filters (as in reference 5).

3.3. Fourier domain filtering

The relation : $\mathbf{S_{meas}} = \mathbf{S} * *\mathbf{h}$ can be easily transposed in Fourier domain : $\tilde{\mathbf{S}}_{\mathbf{meas}} = \tilde{\mathbf{S}} \cdot \tilde{\mathbf{h}}$, where the tilde sign indicates the Fourier transform ($\tilde{\mathbf{S}} = \mathscr{F}\{\mathbf{S}\}$). In Fourier domain, the convolution was replaced by a multiplication. Therefore, the Fourier transform of the unknown, scattering-free signal can be expressed as :

$$\tilde{\mathbf{S}} = \tilde{\mathbf{S}}_{\mathbf{meas}} / \tilde{\mathbf{h}} = \tilde{\mathbf{S}}_{\mathbf{meas}} \cdot \tilde{\mathbf{I}} \tag{7}$$

from which $\mathbf{S}$ is recovered by the inverse Fourier transform of $\tilde{\mathbf{S}}$.

Those considerations show that scattering compensation in Fourier domain is possible, and that the computation cost per 3D frame corresponds to two Discrete Fourier Transforms (DFT), and a division of two complex images.

4. SCATTERING MODELS

The scattering model presented above implies that scattering can be described as a convolution operation with a PSF that models the real-world camera response. However, the PSF $\mathbf{\Delta h}$ is not known a-priori. In the following section, we present several variant scattering descriptors and discuss their use for scattering compensation.

4.1. Scattering descriptors

4.1.1. PSF from real-world measurement

Ideally, the construction of a scattering model should be based on a real-world measurement of the scattering PSF $\Delta h(i,j)$ However, this approach is not practical, for two main reasons :

- a real-world scene where exactly one pixel of the camera sensor is in the foreground is practically impossible to set up.
- the values of the PSF are very small and their measurement is subject to noise.

Those two elements push toward a scattering description where the PSF can be described as an analytical function depending on few parameters.

4.1.2. PSF as sum of gaussians

Using gaussians as building blocks allows to ensure that the scattering PSF $\Delta h(i,j)$ decreases when the separation between the anchor point and pixel (i,j) is large. Using anisotropic gaussian kernels allows to model the asymmetry observed between sensor rows and sensor columns. But the main advantage of the sum of gaussians approach is that only a small number of parameters require to be optimized. If the number of gaussians is set to G, the number of free parameters is equal to $3 \cdot G$. Explicitly, for each gaussian, the width of the gaussian, both in the horizontal and the vertical direction need to be determined, along with a scalar amplitude factor. The PSF $\mathbf{\Delta h}$ is then defined as

$$\Delta h(i,j) = \sum_{k=1}^{G} \mathbf{g}(k) = \sum_{k=1}^{G} w(k) \cdot h_h(i,k) \cdot h_v(j,k) \tag{8}$$

where :

- $\mathbf{h_h}$ is a 1D horizontal gaussian kernel($\in \mathbb{R}$): $h_h(i,k) = \frac{1}{\sqrt{2\pi}\sigma_h(k)} e^{-\frac{i^2}{2\sigma_h^2(k)}}$
- $\mathbf{h_v}$ is a 1D vertical gaussian kernel ($\in \mathbb{R}$): $h_v(j,k) = \frac{1}{\sqrt{2\pi}\sigma_v(k)} e^{-\frac{j^2}{2\sigma_v^2(k)}}$
- $w(k)$ is a scalar ($\in \mathbb{R}$) weight.
- G is the count of gaussian kernels used in the model.

For commodity of notation, we will designate by Θ the set of $3 \cdot G$ parameters that specify a given PSF model.

4.1.3. Inverse filter

For scattering compensation by image domain filtering, a description of the inverse filter $\mathbf{\Delta I}$ is required. When a model for the scattering PSF $\mathbf{\Delta h}$ is known, the inverse filter can be determined from relation 6. In the general case, the inverse filter is a discrete function $\Delta I(i,j)$, which can not be separated for faster computation.

4.1.4. Inverse filter expressed as sum of gaussians

Using a description of the inverse filter $\mathbf{\Delta I}$ as a sum of gaussian kernels ($\mathbf{\Delta I} = \sum \mathbf{g}$) allows to significantly reduce the computation cost for scattering compensation through image domain filtering.[5]

4.2. Computation load for scattering compensation

Table 1 shows a comparison of the computational complexity for approaches of deconvolution (image domain or Fourier domain filtering), and for different scattering descriptors. The image space filtering approach is practical only if the inverse filter is expressed as a sum of separable gaussians. Nevertheless, the complexity is higher than in Fourier transform processing. Finally, the Fourier domain filtering is preferred since it involves the lowest complexity of computation, independently of the scattering descriptor used.

Among the descriptors, the PSF expressed as sum of gaussians ($\mathbf{\Delta h} = \sum \mathbf{g}$) is preferred since it directly describes the phenomenological scattering model of fig. 2, and since it is specified by a small set of parameters Θ that may be easily optimized.

Table 1. Comparison of deconvolution complexity for different scattering models

		Image domain filtering	**Fourier domain filtering**
Scattering descriptor	• $\Delta h(i,j)$ • $\mathbf{\Delta h} = \sum \mathbf{g}$ • $\Delta I(i,j)$	Complexity $\mathscr{O}\left(M^2N^2\right)$	Complexity $\mathscr{O}\left(MN(log(MN))\right)$.
	• $\mathbf{\Delta I} = \sum \mathbf{g}$	Complexity $\mathscr{O}\left(MN(M+N)\right)$.	

4.3. Method for model estimation

The experimental setup for measuring the model consists in the recording of two range images, the first from an arbitrary scene named background, the second from the same scene with an additional object close to the camera named foreground. The basic idea for estimating the parameters Θ of the PSF $\mathbf{\Delta h}(\Theta)$ that best describes the real camera consists in varying $\mathbf{\Delta h}(\Theta)$ until a best match is found between the scattering compensation of the foreground image and the background image.

4.3.1. Experimental setup

A schematic description of the measurement setup is given in fig. 3. This metric requires a set of two TOF measurements of the same background scene. In the first measurement (fig. 3**(a)**), the range image for the background scene $\mathbf{r_{bg}}$ is recorded. In the second measurement (fig. 3**(b)**) a close object causing strong scattering is introduced in the field of view, and the foreground image $\mathbf{r_{meas}}$ is recorded. The scattering compensation algorithm can then be applied to the foreground image (fig. 3**(d)**), producing the compensated image $\mathbf{r_{comp}}$.

Quantitative comparison is performed on the images excluding scatterer*(fig. 3**(c)**). The depth error is defined

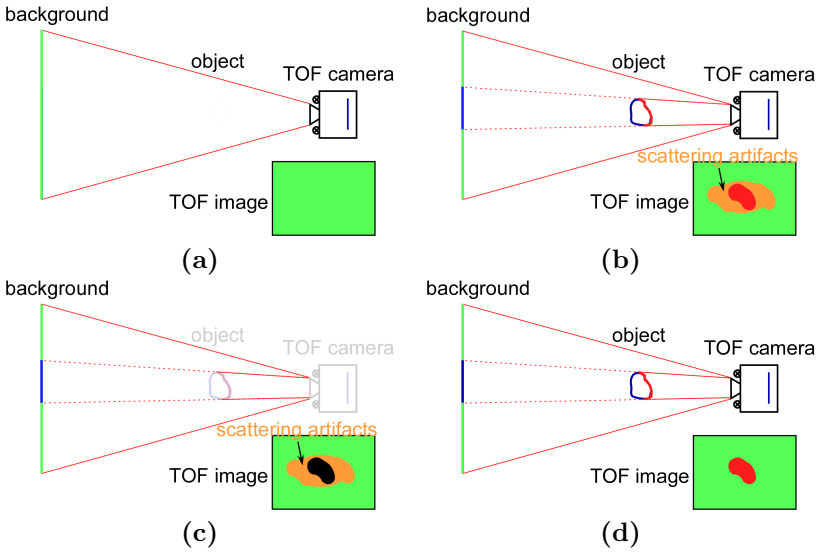

Figure 3. Experiment setup for scattering quantification. **(a)** : Background measurement $\mathbf{r_{bg}}$- **(b)** : Measurement with foreground object $\mathbf{r_{meas}}$ - **(c)** : Background only image for foreground scene $\mathbf{r_{meas,masked}}$ - **(d)** : Output with scattering compensation $\mathbf{r_{comp}}$

as the average :

$$E(\mathbf{r}) = \sum_{(i,j)\in background} |r(i,j) - r_{bg}(i,j)| \,/ \sum_{(i,j)\in background} 1 \tag{9}$$

This quantity can be interpreted as the average displacement for backgrounds pixel in the range image $\mathbf{r}$.

4.3.2. Parameter estimation by human expert

A straightforward method for improvement of scattering compensation results is the estimation of parameters Θ through trial and error by a human expert. Proceeding by trial and error, it is possible to quickly determine a set of parameters which allow for a large reduction in scattering artifacts.

4.3.3. Strategy for model improvement

The quality of the parameters Θ used can be quantified by monitoring the error $E(\mathbf{r_{comp}})$ as Θ is varied. The set of parameters used is optimal if the error after compensation $E(\mathbf{r_{comp}})$ is minimized.

5. EXPERIMENTS

In this section, we apply the proposed scattering compensation methods to a series of range images and compare performances in terms of computational cost and residual compensation error.

5.1. Processing speed

Table 2 compares the processing time for 4 different scattering compensation implementations, running on the same computer, and producing identical results:

- Image domain filtering with discrete function $\Delta I(i,j)$
- Image domain filtering with inverse filter expressed as a sum of separable gaussians ($\mathbf{\Delta I} = \sum \mathbf{g}$)
- Image domain filtering with inverse filter $\mathbf{\Delta I}$ expressed as a sum of separable gaussians, realized with optimized image processing library (IPL 2.5)[9]
- Fourier domain filtering with PSF $\mathbf{\Delta h}$

Table 2. Average processing time for different scattering descriptors.

	Image domain filtering			**Fourier domain filtering**
	Discrete function $\Delta I(i,j)$	**Sum of gaussians** $\mathbf{\Delta I} = \sum \mathbf{g}$	**Optimized sum of gaussian** $\mathbf{\Delta I} = \sum \mathbf{g}$	$\mathbf{\Delta h} = \sum \mathbf{g}$
Complexity	$\mathcal{O}\left(M^2N^2\right)$	$\mathcal{O}\left(MN(M+N)\right)$	$\mathcal{O}\left(MN(M+N)\right)$	$\mathcal{O}\left(MNlog(MN)\right)$
Average proc. time per frame	46.0 s	0.460 s	0.085 s	**0.033 s**

The comparison clearly verifies that Fourier domain processing allows for faster scattering compensation. Moreover, it should be remembered that Fourier domain processing is the only usable method where the PSF $\mathbf{\Delta h}$ can be directly parametrized as a sum of gaussians.

5.2. Compensation performance

5.2.1. Parameter determination by trial and error for gaussian weights

The influence of the PSF parameters Θ used on the different errors is expressed only as a result from convolution operations. Therefore, no simple functional relation between the set of parameters Θ and the error $E\left(\mathbf{r_{comp}}\right)$ is not available. As a consequence, empirical optimization through trial and error is preferred, although it does not provide a guarantee concerning the optimality of a given set of parameters Θ. Seeking optimality would require to perform an exhaustive search of the parameter space. Unfortunately, exhaustive search is too long to be practical, even for simple parametric model for the PSF. A further simplification is therefore required.
Using a small sum of gaussians to model the PSF (one to three gaussians), and a fixed width for each gaussian (the widths are fixed by a human expert, who takes into account the requirement to compensate scattering on different spatial scales) allows to coarsely span the parameter space of the scalar weights associated with each gaussian kernel in a reasonable amount of time. During this search, the error $E\left(\mathbf{r_{comp}}\right)$ is monitored.

The set of parameters used in fig. 4 was obtained after a coarse search of the best compensation results for a model with three gaussians, of fixed geometry (see table 3). As described in section 4.3.3, only the weights

Table 3. Width for the individual gaussians used in optimization experiment.

g	σ_h	σ_v
1	32	64
2	48	48
3	64	64

associated with each gaussian were modified during the search. The particular search that lead to the choice of model of table 4 involved 343 different weight combinations (7 weights for each gaussian).

5.2.2. Measurement of scattering residuals for SR-3100 camera

Figure 4 shows the result of an experiment of scattering compensation for a scattering model where the PSF $\mathbf{h}$ is expressed as a sum of two gaussians. Again, this example was taken taken according to the protocol defined in section 4.3.1 : $\mathbf{r_{bg}}$ is the background range image, $\mathbf{r_{meas}}$ is the measured foreground range image, and $\mathbf{r_{comp}}$ is the foreground range image after scattering compensation. For each range image (4**(c)**,**(e)**), a masked difference image is also provided to highlight depth artifacts (4**(d)**,**(f)**). Although the result after compensation is not yet ideal, it does nevertheless show a significant improvement over the raw measurement. As mentioned above, this improvement is important for applications where the background of the range scene must be monitored. This result was obtained with a PSF $\mathbf{\Delta h}$ defined as the sum of two gaussians (see table 4). In the example presented above, using the compensation algorithm allowed to reduce scattering by an amount corresponding to more that 75% of its original value.

*an *ad-hoc* segmentation scheme on $\mathbf{r_{meas}}$ is used to identify scatterer pixels

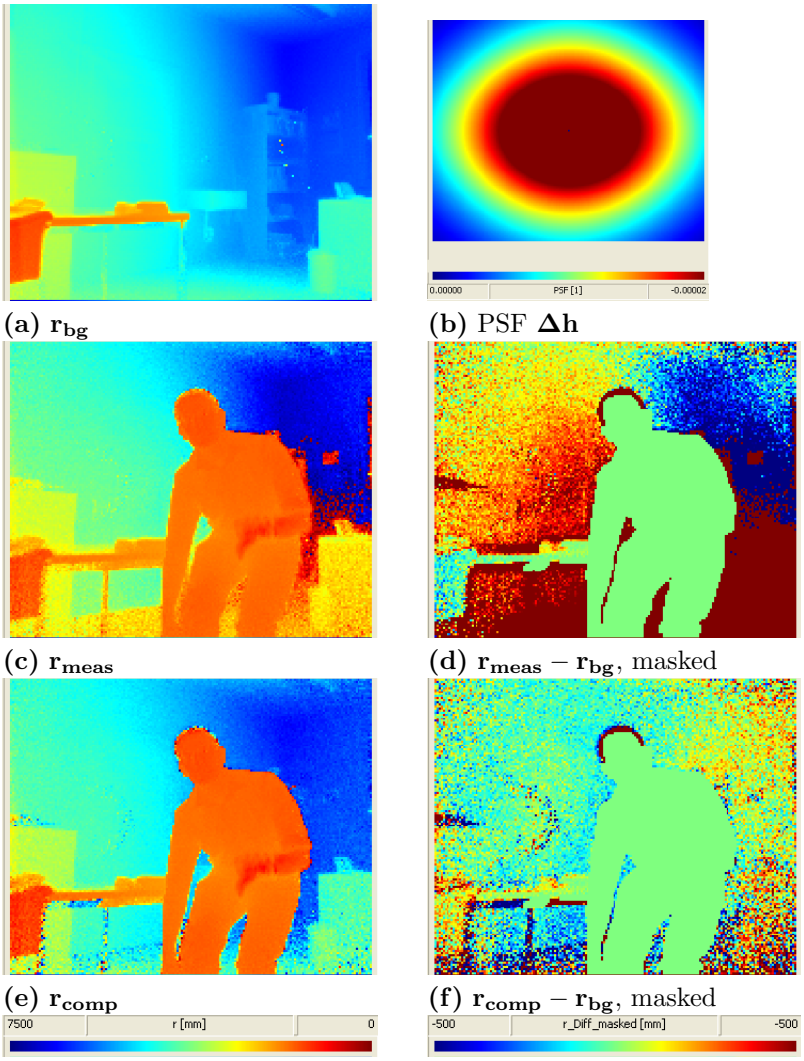

(a) $\mathbf{r_{bg}}$ (b) PSF $\mathbf{\Delta h}$

$E(\mathbf{r_{bg}}) = \mathbf{0}$mm

(c) $\mathbf{r_{meas}}$ (d) $\mathbf{r_{meas}} - \mathbf{r_{bg}}$, masked

$E(\mathbf{r_{meas}}) = \mathbf{747}$mm

(e) $\mathbf{r_{comp}}$ (f) $\mathbf{r_{comp}} - \mathbf{r_{bg}}$, masked

$E(\mathbf{r_{comp}}) = \mathbf{172}$mm

Figure 4. Scattering compensation experiment; the background scene is an office room, the foreground object a person walking in the room.

Table 4. PSF model used for SR-3100 camera.

g	σ_h	σ_v	w
1	32	64	+0.1333
2	48	48	+0.2800

5.3. Qualitative comparison of depth images

Figure 5 shows a small collection of range images illustrating scattering compensation results. Range is represented by a color code, from red (close to the camera) to blue (far from the camera). Those examples were taken according to the protocol defined in section 4.3.1.$\mathbf{r_{bg}}$ is the background range image, $\mathbf{r_{meas}}$ is the measured foreground range image, and $\mathbf{r_{comp}}$ is the foreground range image after scattering compensation. In all

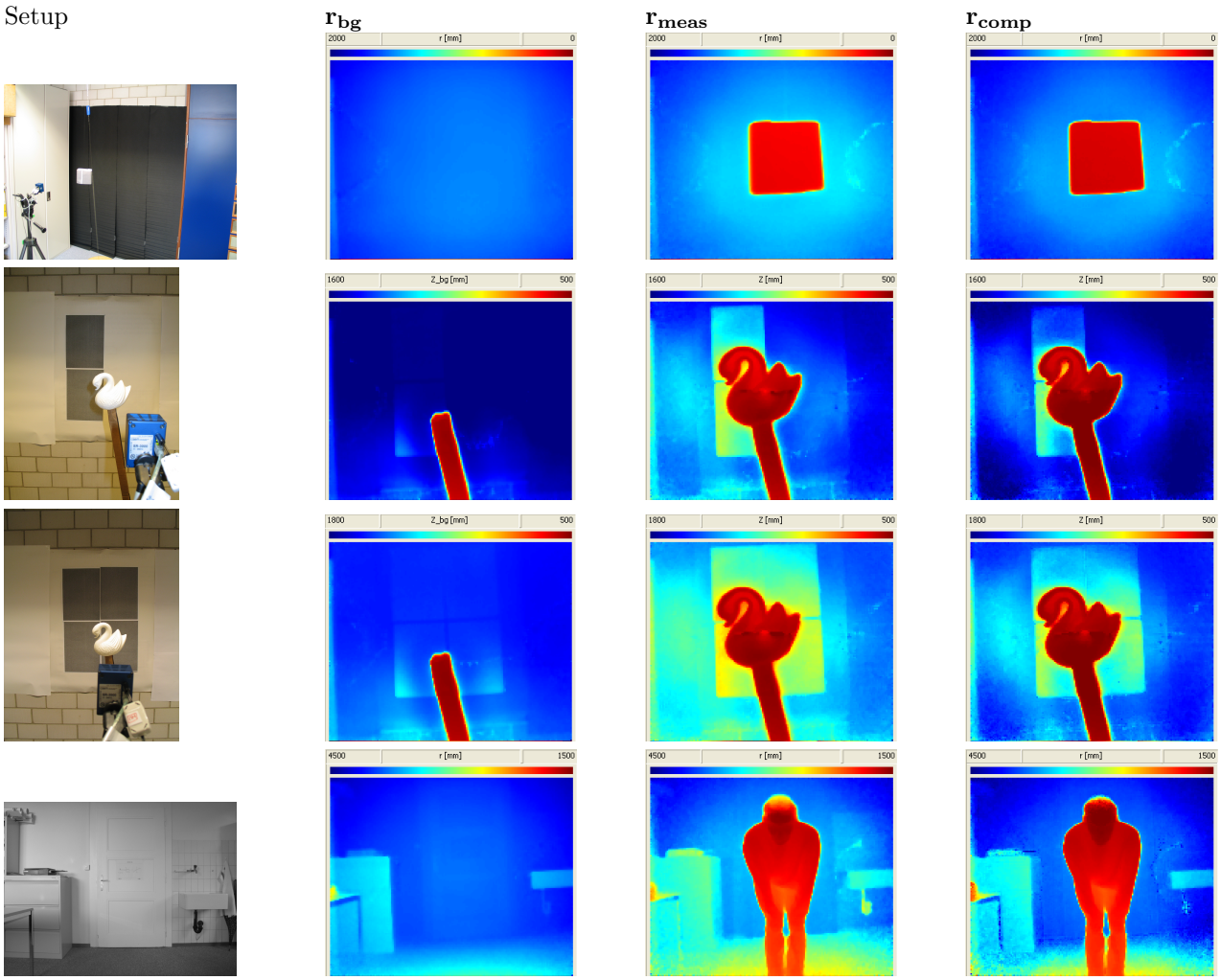

Figure 5. Scattering compensation experiments. $\mathbf{r_{bg}}$ is the background range image, $\mathbf{r_{meas}}$ is the measured foreground range image, and $\mathbf{r_{comp}}$ is the foreground range image after scattering compensation.

situations shown, scattering artifacts are very strong : they are easily recognizable on a color map showing depth difference for several *meters*. In those situations, the result with scattering compensation is not perfect : some range values for background pixels are still highly different in the image with the object, when compared with the background image. Unfortunately, scattering compensaton performance is strongly dependent on the scene imaged. Nevertheless, tests performed so far have shown that scattering compensation always brings a significant improvement: between 38% in adverse situations up to 95% in favorable situations.

6. CONCLUSION

The paper is a contribution to the reduction of scattering in TOF cameras. First, a simple physical model for scattering was used and scattering compensation algorithms were investigated. Two algorithms implementations

were compared, and it was shown that scattering compensation performed in Fourier domain offers the best performance, in processing time, but also in commodity of usage relative to the specific scattering description used in the model. We observed that the most useful description of scattering is the PSF $\mathbf{\Delta h}$, since it provides a description which is close to the phenomenon occurring inside the camera device.

Then, given that a direct PSF measurement cannot be performed because of noise, a parametric description for the PSF was introduced, in the form of a sum of gaussians. The PSF is estimated by trial and error. An error metric allowing to compare results from different scattering models was defined, and a semi-automated parameter determination process was presented.

Then also the effectiveness of the proposed scattering reduction algorithm was tested on many different scenes. The improvement varied between 38% in adverse situations up to 95% in favorable situations. The computation cost is in the order of $30ms$, which is sufficiently low for many high frame rate applications.

Finally, we believe that for improved scattering compensation, more advanced models of the scattering phenomenon should be used. Experiments suggest that the hypothesis of a space invariant PSF for scattering is not fully verified. Advanced scattering compensation algorithms could involve models with different PSFs depending on the position of the scatterer object in the field of view, or on its distance to the camera.

ACKNOWLEDGMENTS

This work was supported by the Swiss Federal Innovation Promotion Agency KTI/CTI (Projet no. 7719.1 ESPP-ES).

REFERENCES

1. CSEM, "Swissranger SR-3000 manual v1.02," June 2006. http://www.swissranger.ch/customer.
2. T. Kahlmann, F. Remondino, and H. Ingensand, "Calibration for Increased Accuracy of the Range Imaging Camera SwissRanger," in *Proc. of the ISPRS Com. V Symposium*, pp. 136–141, ISPRS, sep 2006.
3. N. Santrac, G. Friedland, and R. Rojas, "High Resolution Segmentation with a Time-of-flight 3D-Camera using the Example of a Lecture Scene," Sept. 2006. Technical report, available from: http://www.inf.fu-berlin.de/inst/ag-ki/eng/index.html.
4. T. Kahlmann and H. Ingensand, "Increased accuracy of 3D range imaging camera by means of calibration," in *Proc. of the 8th Conference on Optical 3D Measurements*, pp. 101–108, july 2007.
5. J. Mure-Dubois and H. Hügli, "Real-time scattering compensation for time-of-flight camera," in *Proc. of the ICVS 2007*, ICVS, Feb 2007.
6. CSEM, "Swissranger," 2006. http://www.swissranger.ch.
7. PMD Technologies., "Pmdvision," 2006. http://www.pmdtec.com/e_index.htm.
8. Canesta Inc., "Canestavision," 2006. http://www.canesta.com/index.htm.
9. Intel Inc., "Intel Image Processing Library 2.5," 2000. http://developer.intel.com/software/products/perflib/.